

## Two-Component Duality and Fixed- $t$ Dispersion Relations for $\pi^-p \rightarrow \pi^0n$

R. C. E. Devenish and B. R. Martin

*Department of Physics and Astronomy, University College London, London, England WC1E 6BT*

(Received 15 March 1973)

Pion-nucleon charge-exchange data below 2 GeV/c have been fitted using fixed- $t$  dispersion relations, and the hypothesis of two-component duality. Good fits were obtained, and the resulting amplitudes are in agreement with recent phase-shift analyses. Predictions for the crossing-even amplitudes are shown to be compatible with experiment.

### I. INTRODUCTION

In this paper we present an analysis of low-energy data for  $\pi^-p \rightarrow \pi^0n$ , using fixed- $t$  dispersion relations and the ideas of duality. More specifically, we use the hypothesis of two-component duality,<sup>1</sup> which is the statement that high-energy Regge poles are dual (in the sense of finite-energy sum rules) to low-energy resonances, and the Pomeron is dual to the background remaining after the resonances are subtracted from the full amplitude.

Qualitative evidence in support of this hypothesis comes from the work of Harari and Zarmi,<sup>2</sup> who used  $\pi N$  phase shifts to construct  $s$ -channel amplitudes with definite  $t$ -channel isospins. The results showed that resonances in amplitudes corresponding to  $I_t = 1$  exchange were accompanied by far smaller backgrounds than those in amplitudes corresponding to  $I_t = 0$ . Similar evidence has been presented for  $KN$  scattering.<sup>3</sup> It follows that reactions corresponding to isospin exchange in the  $t$  channel should be resonance saturated at low energies, and this assumption has been used to analyze  $\pi N$  CEX (charge-exchange) data.<sup>4</sup> However, prior analyses assumed resonance dominance for both the real and imaginary parts of the amplitude which is unreasonable, since it is only the imaginary part of a resonance which is a local effect; the real part vanishes at resonance, and is non-negligible some distance from the resonance. Thus, from FESR (finite-energy sum rules) arguments, only the imaginary parts of such amplitudes are expected to be resonance dominated. Given the imaginary part, however, the real part can be calculated from fixed- $t$  dispersion relations and this is the method we will employ.

The use of fixed- $t$  dispersion relations in phenomenological analyses of low-energy reactions is long-established. Some examples are the extraction of threshold parameters for  $\pi N$  (Ref. 5) and  $KN$  (Ref. 6) scattering, and the construction of models for low-energy pion electroproduction.<sup>7</sup> More recently, fixed- $t$  dispersion relations have

been used in conjunction with duality to calculate high-energy amplitudes for  $\pi^-p \rightarrow \pi^0n$  (Refs. 8 and 9) and  $\gamma N \rightarrow \pi N$  (Ref. 10). The inputs for all these calculations are (among other things) low-energy amplitudes, usually taken from partial-wave (phase shift and multipole) analyses. Far less work has been done using the fixed- $t$  dispersion relations to extract such amplitudes directly from data, although some analyses have been made.<sup>11,12</sup> By combining the use of fixed- $t$  dispersion relations with the two-component duality hypothesis, we are able to construct an economical, but theoretically satisfactory, parametrization which is particularly suitable for analyzing inelastic reactions in situations where data are few, but the resonance spectrum (i.e., masses and total widths) is reasonably well known. Thus, for example, resonance coupling (partial widths) could be obtained from reactions such as  $\pi N \rightarrow \eta N$ ,  $\pi N \rightarrow K\Lambda$ , and  $\gamma N \rightarrow K\Lambda$ .

To test whether such a model is capable of producing *quantitatively* satisfactory results, we have analyzed data for  $\pi^-p \rightarrow \pi^0n$  in the region below 2 GeV/c, as this is a reaction where much information already exists from  $\pi N$  phase-shift analyses.

### II. FIXED- $t$ DISPERSION RELATIONS

We use the standard  $\pi N$  invariant amplitudes  $A^\pm(s, t)$ ,  $B^\pm(s, t)$ ,<sup>5</sup> and

$$A'^\pm(s, t) \equiv A^\pm(s, t) + \frac{M(s-u)}{4M^2-t} B^\pm(s, t). \quad (2.1)$$

The crossing-odd amplitudes are related to those for  $\pi^-p \rightarrow \pi^0n$  by

$$A_{\text{CEX}} = -\sqrt{2} A^-, \quad B_{\text{CEX}} = -\sqrt{2} B^-,$$

and obey unsubtracted fixed- $t$  dispersion relations of the form<sup>5</sup>

$$\text{Re}A^-(\nu, t) = \frac{P}{\pi} \int_{\nu_0}^{\infty} d\nu' \text{Im}A^-(\nu', t) \left( \frac{1}{\nu' - \nu} - \frac{1}{\nu' + \nu} \right), \quad (2.2)$$

and

$$\begin{aligned} \operatorname{Re} B^-(\nu, t) &= \frac{G^2}{2M} \left( \frac{1}{\nu_B - \nu} + \frac{1}{\nu_B + \nu} \right) \\ &+ \frac{P}{\pi} \int_{\nu_0}^{\infty} d\nu' \operatorname{Im} B^-(\nu', t) \left( \frac{1}{\nu' - \nu} + \frac{1}{\nu' + \nu} \right), \end{aligned} \quad (2.3)$$

where

$$\begin{aligned} \nu &\equiv \frac{(s-u)}{(4M)}, \\ \nu_0 &= \mu + \frac{t}{4M}, \\ \nu_B &= \frac{-\mu^2}{2M} + \frac{t}{4M}, \end{aligned}$$

$\mu$  is the pion mass, and  $G^2$  the  $\pi NN$  coupling constant. The unsubtracted dispersion relation for  $A'^-(\nu, t)$  follows from Eqs. (2.1) - (2.3). These relations are valid in principle for all physical values of  $t$ . However, for a fixed value of  $t$  we require the imaginary parts for all  $\nu_0 \leq \nu < \infty$ , and part of this range will, in general, be unphysical. We have evaluated this in the standard way by using the usual Legendre expansions to extrapolate the low- $\nu$  amplitudes to unphysical  $t$  values. Examination of the nearest double spectral functions suggests that this expansion should be valid at least to  $|t| \lesssim 1 \text{ GeV}^2 = 50\mu^2$ . Another reason for restricting  $t$  to this range is that we will be evaluating the high-energy part of the integrals using a Regge-pole model, the parameters of which are only well-determined for  $|t| \lesssim 50\mu^2$ .

#### A. Low-Energy Input

In the spirit of the two-component duality hypothesis, we use resonances *alone* as the low-energy input to the integrals of the dispersion relations. The form we use for the partial-wave amplitudes of definite isospin is

$$\operatorname{Im} f_{l\pm}(s) = \frac{1}{q} \frac{x(\frac{1}{2}\Gamma)^2}{(W_R - W)^2 + (\frac{1}{2}\Gamma)^2}, \quad (2.4)$$

where  $W_R$  is the mass,  $\Gamma$  the total width,  $x$  the elasticity, and  $W = \sqrt{s}$ . To maintain the correct threshold behavior of  $\operatorname{Im} f_{l\pm}(s)$ , the width  $\Gamma(q)$  must contain a factor  $q^{2l+1}$  close to threshold, but away from this region the form of  $\Gamma(q)$  is somewhat arbitrary. Certainly, to use the  $q^{2l+1}$  factor above the resonance energy would be unreasonable, as the high-energy behavior would not be expected to be controlled by a threshold condition. In prac-

tice we have investigated three widely-used models for  $\Gamma(q)$ . These are shown in Table I.<sup>2,13,14</sup>

The resonance form (2.4), with  $\Gamma(q)$  given by one of the models of Table I, was used for all resonances except the  $N^*(1232)$ . The latter was treated as a fixed contribution of the form

$$\operatorname{Im} f_{l+}(s) = \frac{c^2 q^5}{(q^2 - q_R^2)^2 (1 + a^2 q^2)^2 + c^2 q^6},$$

which gives a good fit to the  $P_{33}$  phase shift of Carter *et al.*,<sup>15</sup> with the parameters,  $a^2 = 21.4 \text{ GeV}^{-2}$ ,  $c = 4.27 \text{ GeV}^{-1}$ ,  $q_R^2 = 0.0508 \text{ GeV}^2$ .

#### B. High-Energy Input

We treat the high-energy part of the dispersion relations as a fixed contribution, and evaluate it by a Regge-pole model. The model we use is the five-pole fit of Barger and Phillips,<sup>16</sup> (i.e.,  $P$ ,  $P'$ ,  $P''$ ,  $\rho$ , and  $\rho'$ ), which for the crossing-odd amplitudes gives

$$\operatorname{Im} A'^-(\nu, t) = -\nu \sum_{i=\rho, \rho'} \gamma_i \cos(\frac{1}{2}\pi\alpha_i) (\nu^2 - \nu_0^2)^{\alpha_i - 1/2},$$

$$\operatorname{Im} B^-(\nu, t) = -\sum_{i=\rho, \rho'} \beta_i \cos(\frac{1}{2}\pi\alpha_i) (\nu^2 - \nu_0^2)^{\alpha_i - 1/2}.$$

(The precise forms for the trajectory and residue functions are given in Ref. 16.) The parameters of this model were obtained by fitting data above about  $4.5 \text{ GeV}/c$ , but the model still gives a good fit to the data when extrapolated down to  $\approx 2 \text{ GeV}/c$ . Evidence for its correctness comes from an amplitude analysis of 6- $\text{GeV}/c$   $\pi N$  data,<sup>17</sup> the results of which are well reproduced by the model.

#### C. $\pi N$ Charge-Exchange Data

The pion-nucleon charge-exchange data that we fitted consist of 620 differential cross sections (for  $|t| < 50\mu^2$ ) at 81 separate momenta between

TABLE I. Parametrizations for  $\Gamma(q)$ .  $\Gamma_R$  is a constant and  $q_R$  is the value of the momentum  $q$  at resonance.

Model	$q < q_R$	$q > q_R$	Comments
a	$\Gamma_R \left( \frac{q}{q_R} \right)^{2l+1}$	$\Gamma_R$	Used, for example, by Harari and Zarmi <sup>2</sup>
b	$\Gamma_R \left( \frac{q}{q_R} \right)^{2l+1}$	$\left( \frac{q_R^2 + x^2}{q^2 + x^2} \right)^l$	$x = 2.5\mu$ , used, for example, by Walker <sup>13</sup>
c	$\Gamma_R \left( \frac{q}{q_R} \right)^{2l+1}$	$\frac{D_l(q_R r)}{D_l(qr)}$	$D_l$ is the barrier factor of Blatt and Weisskopf, <sup>14</sup> $r = 0.45\mu^{-1}$ .

0.31 GeV/c and 2.07 GeV/c.<sup>18</sup> This is part of the data set used in a recent  $\pi N$  phase-shift analysis,<sup>19</sup> and we have used the same renormalizations as used in that work. In addition, we have fitted the total cross-section difference

$$\Delta\sigma \equiv \sigma(\pi^+p) - \sigma(\pi^-p),$$

at 29 momenta spread throughout the range. Values for  $\Delta\sigma$  were constructed from tabulated values of the  $\pi^\pm p$  total cross sections.<sup>20</sup> The total number of data points is thus 649.

### III. CHARGE-EXCHANGE SOLUTIONS

The method for finding solutions is as follows: For an initial resonance spectrum parametrized by Eq. (2.4) with a particular model for  $\Gamma(q)$ , we form  $\text{Im}A^-$  and  $\text{Im}B^-$  in the low-energy region by the usual partial-wave series [including fixed contributions from the  $N^*(1232)$ ]. We use the Regge-pole model with fixed parameters to form the imaginary parts in the high-energy region, and then use the dispersion relations to calculate the real parts. The resonance parameters are then

varied to fit the data described above.

The resonance spectrum used was that given in the  $N^*$  review section of the Particle Data Group tables,<sup>21</sup> with the exception of the  $D_{13}(1700)$ , which we omitted as it is not definitely confirmed. There is a total of 20 resonances [including the fixed  $N^*(1232)$ ], with angular momenta up to  $G_{7/2}$ , and masses up to 2150 MeV. Since the highest mass state has a width of  $\approx 340$  MeV, we used the Regge form down to center-of-mass energies of 2.5 GeV. (We have checked that in the region of the matching point the high- and low-energy imaginary parts are of comparable magnitudes.) For the initial trial solution we used the average values quoted in the PDG (Particle Data Group) tables,<sup>21</sup> but because we have considerable information about these parameters from several standard phase-shift analyses, we constrained the parameters  $P_i$  of each resonance to lie absolutely within the range  $P_i \pm \Delta_i$ , when  $\Delta_i$  is the maximum spread in  $P_i$  found by comparing the tabulated value from different phase shifts analyses.<sup>21</sup> (The values of  $\Delta_i$  are somewhat larger than the "errors" quoted by the PDG.<sup>21</sup>)

The initial normalized  $\chi^2$  for all the models of

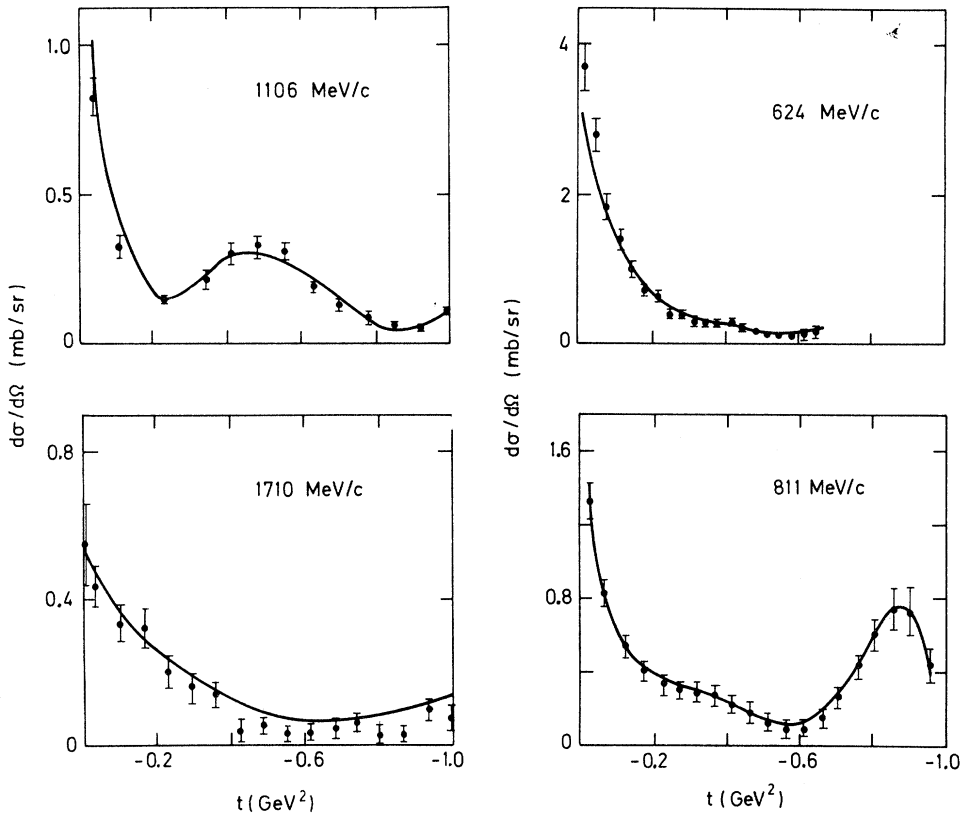


FIG. 1. Fits to some sample charge-exchange differential cross sections obtained from solution (b).

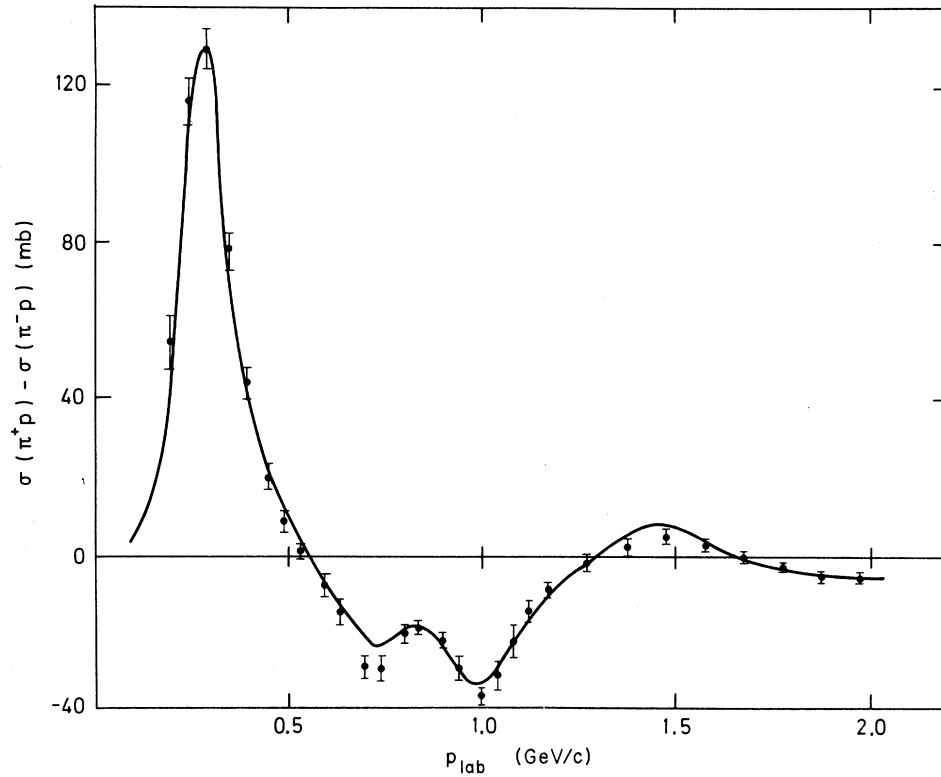


FIG. 2. Fit to  $\Delta\sigma \equiv \sigma(\pi^+p) - \sigma(\pi^-p)$  obtained from solution (b).

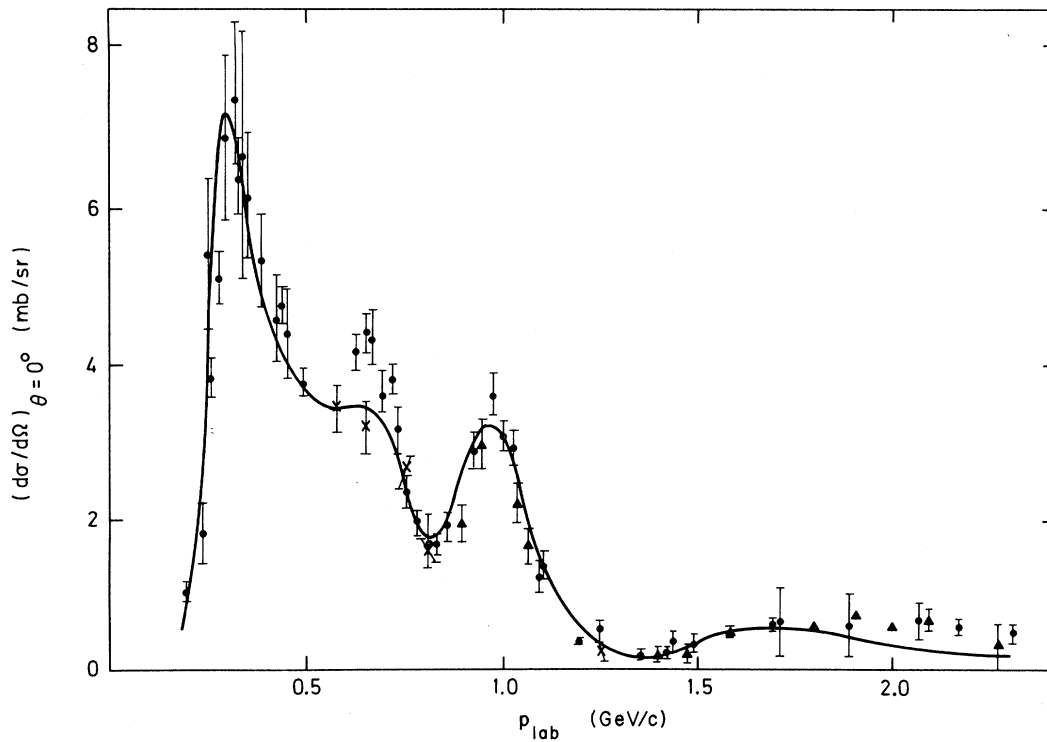


FIG. 3. Fit to the forward charge-exchange differential cross section obtained from solution (b).

TABLE II. Values of the resonance parameters for solution (b). The parameters of the  $P_{33}(1232)$  were kept fixed in the analysis.

$I = \frac{1}{2}$				$I = \frac{3}{2}$			
State	Mass (MeV)	Width (MeV)	$x$	State	Mass (MeV)	Width (MeV)	$x$
$S_{11}'$	1532	65.5	0.32	$S_{31}$	1660	199	0.33
$S_{11}''$	1688	110	0.51	$P_{31}$	1943	200	0.27
$P_{11}'$	1472	291	0.53	$P_{33}'$	1232	113	1.0
$P_{11}''$	1646	142	0.15	$P_{33}''$	1750	185	0.12
$P_{13}$	1808	434	0.19	$P_{33}'''$	2130	290	0.24
$D_{13}'$	1514	130	0.49	$D_{33}$	1649	300	0.18
$D_{13}''$	2029	301	0.26	$D_{35}$	1913	311	0.16
$D_{15}$	1665	175	0.46	$F_{35}$	1913	165	0.15
$F_{15}$	1682	140	0.56	$F_{37}$	1925	209	0.45
$F_{17}$	2001	250	0.12				
$G_{17}$	2148	338	0.33				

$\Gamma(q)$  was  $>20$ , and after minimization fell to 5.6, 3.4, and 3.8 for models (a), (b), and (c), respectively. While model (a) gives a qualitative description of the data, models (b) and (c) give quantitative fits comparable to those obtained in energy-dependent  $\pi N$  phase-shift analysis,<sup>22</sup> and to illustrate this we show in Fig. 1 the predictions of solution (b) compared with some sample differential cross sections, and in Figs. 2 and 3 we show the predictions of the same solution for the cross-section difference  $\Delta\sigma$ , and the forward differential cross section, as functions of energy. The parameters of this solution are given in Table II. To compare this solution in detail with the results of phase-shift analysis, we show in Figs. 4–7  $A_{\text{CEX}}'(\nu, t)$  and  $B_{\text{CEX}}(\nu, t)$  for  $0 \leq |t| \leq 1.0 \text{ GeV}^2$  and  $0 \leq p_{\text{lab}} \leq 2 \text{ GeV}/c$  obtained from solution (b) (solid line), and the same quantities obtained from Ref.

$$\begin{aligned} \text{Re}B^+(\nu, t) = & \frac{G^2}{2M} \left( \frac{1}{\nu_B - \nu} - \frac{1}{\nu_B + \nu} \right) + \frac{1}{\pi} \int_{\nu_0}^{\infty} d\nu' \text{Im}B_R^+(\nu', t) \left( \frac{1}{\nu' - \nu} - \frac{1}{\nu' + \nu} \right) \\ & + \frac{P}{\pi} \int_{\nu_0}^{\nu_c} d\nu' \text{Im}B_{\text{Res}}^+(\nu', t) \left( \frac{1}{\nu' - \nu} - \frac{1}{\nu' + \nu} \right) + \text{Re}B_P^+(\nu, t), \end{aligned} \quad (4.3)$$

where

$$\text{Re}B_P^+(\nu, t) = -\tan\left(\frac{1}{2}\pi\alpha_P\right) \text{Im}B_P^+(\nu, t), \quad (4.4)$$

which follows from the specific form of Eq. (4.2) for the Pomeron. We show in Fig. 8 the values of  $B^+(\nu, t)$  for  $t = 0$  and  $-0.04$  and  $0 \leq p_{\text{lab}} \leq 2 \text{ GeV}/c$  obtained from Eqs. (4.1) and (4.3) using solution (b) as the low-energy resonance input. The agreement with the phase shift results of Almehed and Lovelace<sup>19</sup> is quite satisfactory, despite the fact that no modifications have been made to the Pome-

ron term in the region  $\nu_0 \leq \nu \leq \nu_c$ . For  $A'^+(\nu, t)$ , the two-component duality hypothesis gives for the imaginary part

$$\begin{aligned} \text{Im}A'^+ = & \text{Im}A'_{\text{Res}}^+ + \text{Im}A'_P^+, \quad \nu < \nu_c \\ = & \text{Im}A'_R^+ + \text{Im}A'_P^+, \quad \nu > \nu_c \end{aligned} \quad (4.5)$$

where the Regge pole terms are given by<sup>18</sup>

$$\begin{aligned} \text{Im}A'_i^+(\nu, t) = & \gamma_i \sin\left(\frac{1}{2}\pi\alpha_i\right) (\nu^2 - \nu_0^2)^{\alpha_i/2}, \\ i = & P, P', P''. \end{aligned} \quad (4.6)$$

#### IV. CROSSING-EVEN AMPLITUDES

The fit to the CEX data determines the resonance couplings, but only in the combination  $(A^{3/2} - A^{1/2})$ . Thus, it is necessary to check that the predictions for the crossing-even amplitudes are compatible with experiment. This prediction is not, however, unambiguous, as we now need a model for the imaginary background, which in the two-component duality hypothesis is the Pomeron.

We consider firstly, the amplitude  $B^+(\nu, t)$  where we have

$$\begin{aligned} \text{Im}B^+ = & \text{Im}B_{\text{Res}}^+ + \text{Im}B_P^+, \quad \nu < \nu_c \\ = & \text{Im}B_R^+ + \text{Im}B_P^+, \quad \nu > \nu_c \end{aligned} \quad (4.1)$$

where  $\nu_c$  corresponds to the matching energy  $W = 2.5 \text{ GeV}$ , and Res, P, and R stand for the contributions from the resonances, the Pomeron, and the sum of other  $I = 0$  Regge poles (i.e.,  $P'$  and  $P''$ ), respectively. Thus, we need the Pomeron contribution for  $\nu_0 \leq \nu < \nu_c$ . As a first approximation we have used the parametrization of Barger and Phillips<sup>16</sup> extrapolated to low energies. The Regge-pole terms of Eq. (4.1) are then given by

$$\begin{aligned} \text{Im}B_i^+(\nu, t) = & \nu\beta_i \sin\left(\frac{1}{2}\pi\alpha_i\right) (\nu^2 - \nu_0^2)^{\alpha_i/2}, \\ i = & P, P', P''. \end{aligned} \quad (4.2)$$

The real part may be calculated from an unsubtracted dispersion relation for  $B^+(\nu, t)$ , which, using Eq. (4.1), may be written

The situation for the real part is more complicated because the dispersion relation for this amplitude requires a subtraction. For  $t=0$  we considered a dispersion relation for the amplitude  $A'^+(\nu, t)$  subtracted once at threshold,

$$\text{Re}A'^+(\nu, 0) = \frac{2(\nu^2 - \mu^2)}{\pi} P \int_{\mu}^{\infty} d\nu' \frac{\nu' \text{Im}A'^+(\nu', t)}{(\nu'^2 - \mu^2)(\nu'^2 - \nu^2)} + \text{Re}A'^+(\mu, 0) + \frac{4G^2 M \mu^2 (\nu^2 - \mu^2)}{[(2M\nu)^2 - \mu^4](4M^2 - \mu^2)}, \quad (4.7)$$

where  $\text{Im}A'^+(\nu, t)$  is given by Eq. (4.5) and the subtraction constant can be evaluated in terms of  $s$ -wave  $\pi N$  scattering lengths.<sup>23</sup>

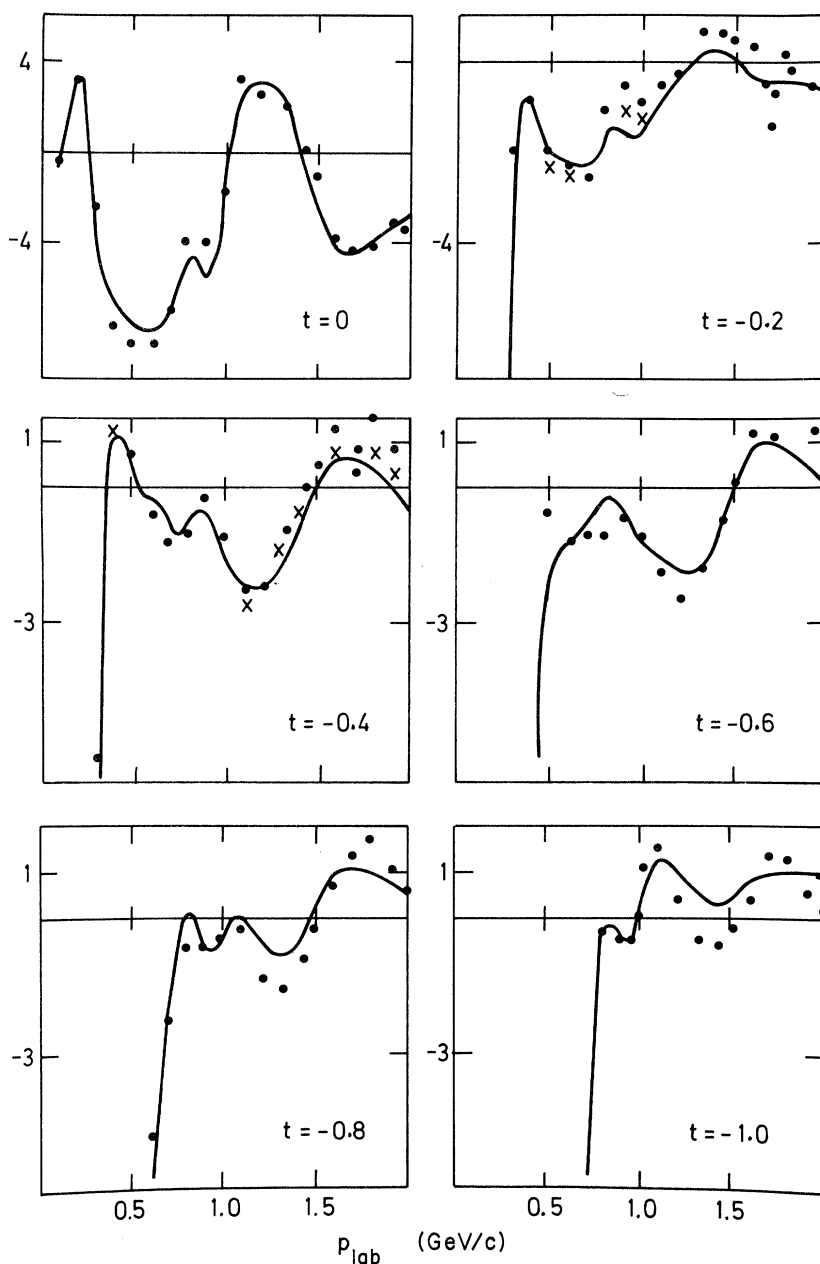


FIG. 4.  $\text{Re}A'_{\text{ex}}(\nu, t)$  at fixed  $t$  (in  $\text{GeV}^2$ ) obtained from solution (b) (solid-lines), from the  $\pi N$  phase shift of Almehed and Lovelace (Ref. 19) (circles), and from the analysis of Pietarinen (Ref. 11) (crosses). (Units:  $\hbar=c=\mu=1.$ )

In Fig. 9(a) we show (dashed curves) values of  $\text{Re}A'^+(\nu, t=0)$  and  $\text{Im}A'^+(\nu, t=0)$  for  $0 \leq p_{\text{lab}} \leq 2$  GeV/c obtained from Eqs. (4.5) and (4.7) using solution (b) as the low-energy resonance input. There is a marked discrepancy between the predictions and the amplitudes obtained from phase-shift analysis,<sup>19</sup> which is due to the extrapolated Pomeron contribution being far too large in the low-energy region. This fact has been noted in previous calculations.<sup>4</sup> However, we are free to

modify the Pomeron contribution, provided the fit to the high-energy data is maintained. As an illustration of this we have modified the Barger-Phillips form for  $\text{Im}A'^+$  by the function  $f(\nu) = 1 - \exp(-np_{\text{lab}}^2)$ , i.e., we have used

$$\text{Im}A'_P(\nu, t) = \gamma_P(\nu^2 - \nu_0^2)^{\alpha_P/2} \sin(\frac{1}{2}\pi\alpha_P) f(\nu). \quad (4.8)$$

With  $n = 0.36 \text{ GeV}^{-2}$ ,  $f(\nu) \approx 1$  for  $p_{\text{lab}} \gtrsim 3 \text{ GeV/c}$ , and

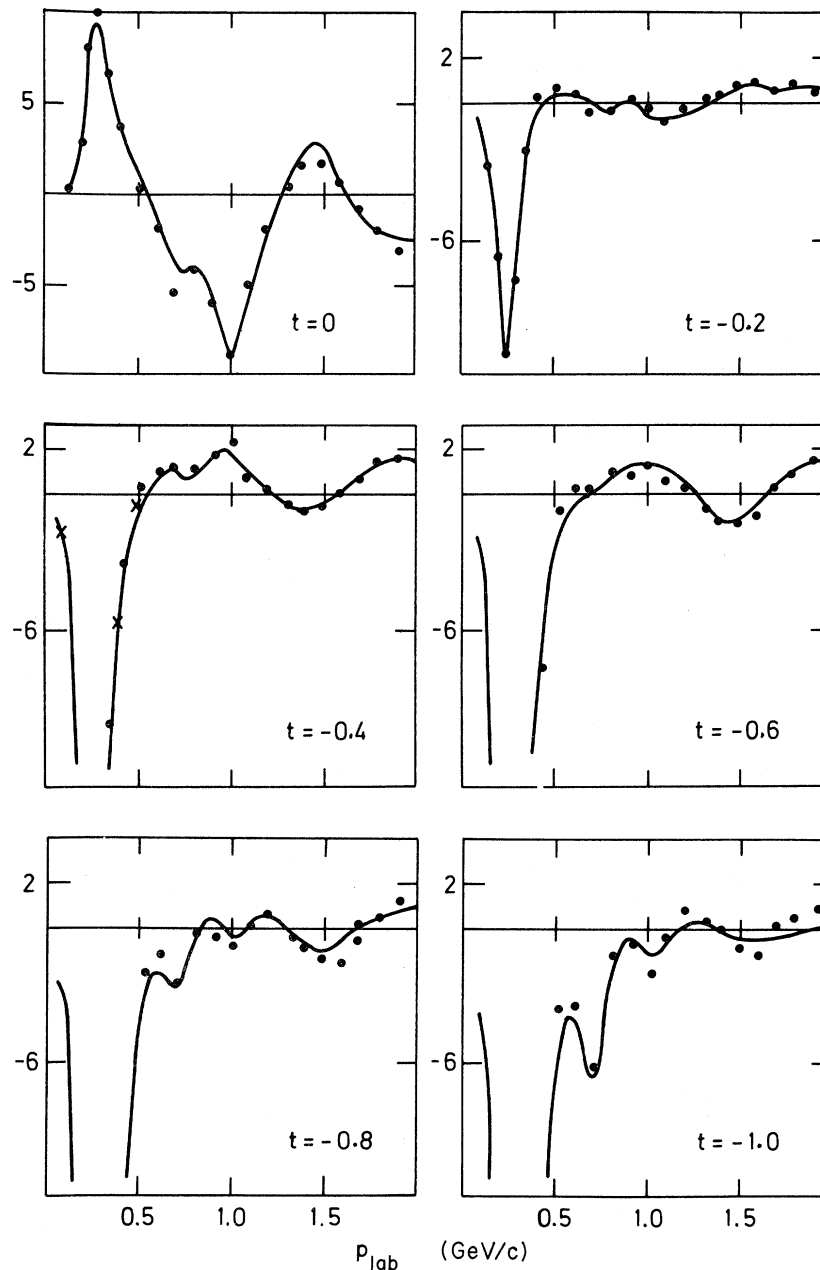


FIG. 5.  $\text{Im}A'_{\text{CEX}}(\nu, t)$  in the notation of Fig. 4.

the original form is recovered.

The solid curves of Fig. 9(a) show the modified predictions for  $\text{Im}A'^+(\nu, t=0)$  and  $\text{Re}A'^+(\nu, t=0)$ , where the latter quantity is again calculated from Eq. (4.7). The agreement between the predictions and the phase-shift solution is now satisfactory except at the highest energies, and this may well be due to neglected higher resonances. For ex-

ample, this discrepancy is approximately halved if the conjectured  $H_{19}(2200)$  and  $H_{311}(2450)$  resonances are included.

For  $t \neq 0$  the subtraction constant  $\text{Re}A'^+(\nu_0, t)$  cannot be evaluated without a knowledge of  $\pi N$  scattering lengths for  $l \geq 1$ . A convergent relation can, however, be obtained by writing an unsubtracted fixed- $t$  dispersion relation for the ampli-

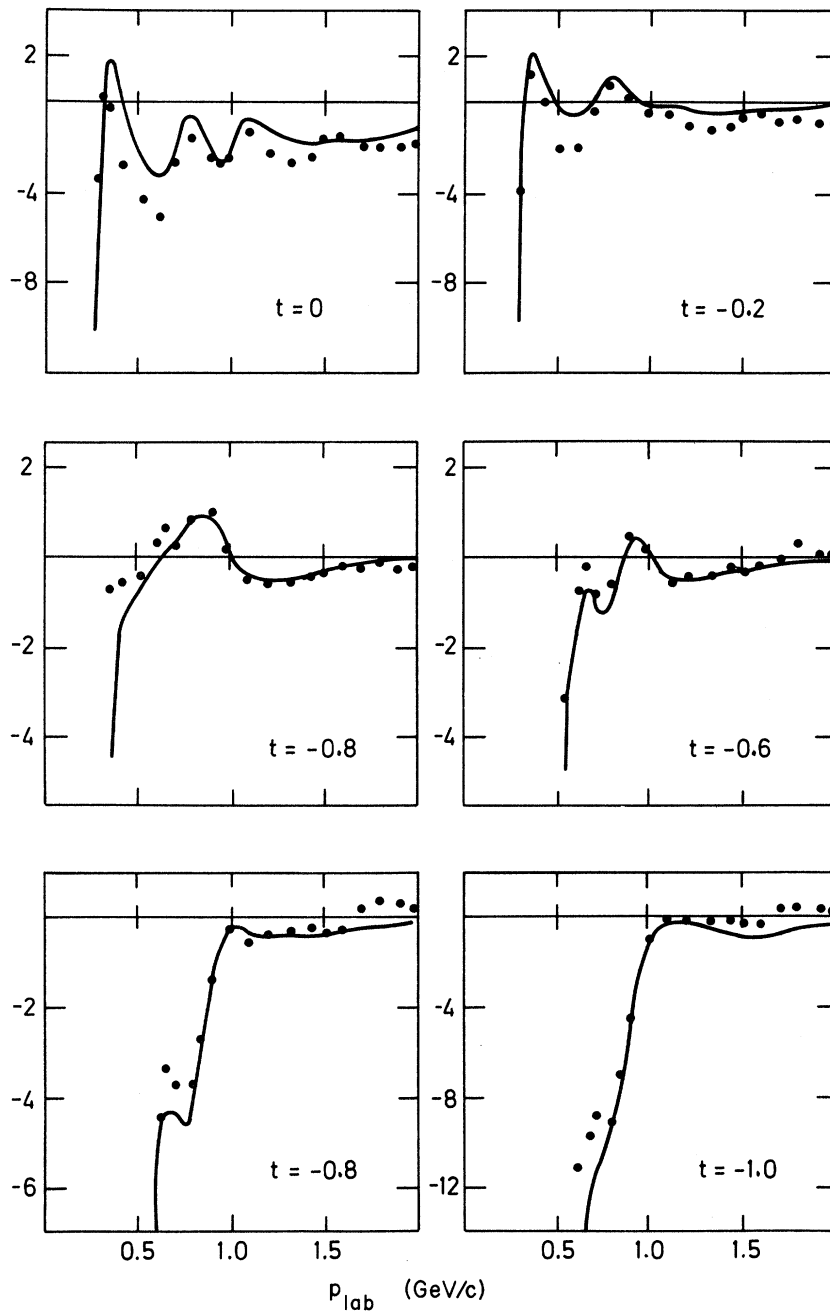


FIG. 6.  $\text{Re}B_{\text{CEX}}(\nu, t)$  in the notation of Fig. 4.



tude<sup>24</sup>

$$\bar{A}^+(\nu, t) \equiv A'^+ - A'_P^+ - A'_{P'}^+.$$

The predictions for  $A'^+(\nu, t = -0.4)$  obtained in this way are shown in Fig. 9(b) using solution (b) as the low-energy resonance input, and the unmodified Pomeron and  $P'$  parametrizations. The agreement with the phase shift solution is not as

good as at  $t = 0$ , but again we have the freedom to modify the Pomeron (and now also the  $P'$ ) contribution.

Finally, we have checked that the real parts of the amplitudes (both crossing-even and crossing-odd) at high energies, calculated from the dispersion relations are in substantial agreement with those given by the fit of Barger and Phillips,<sup>16</sup> and

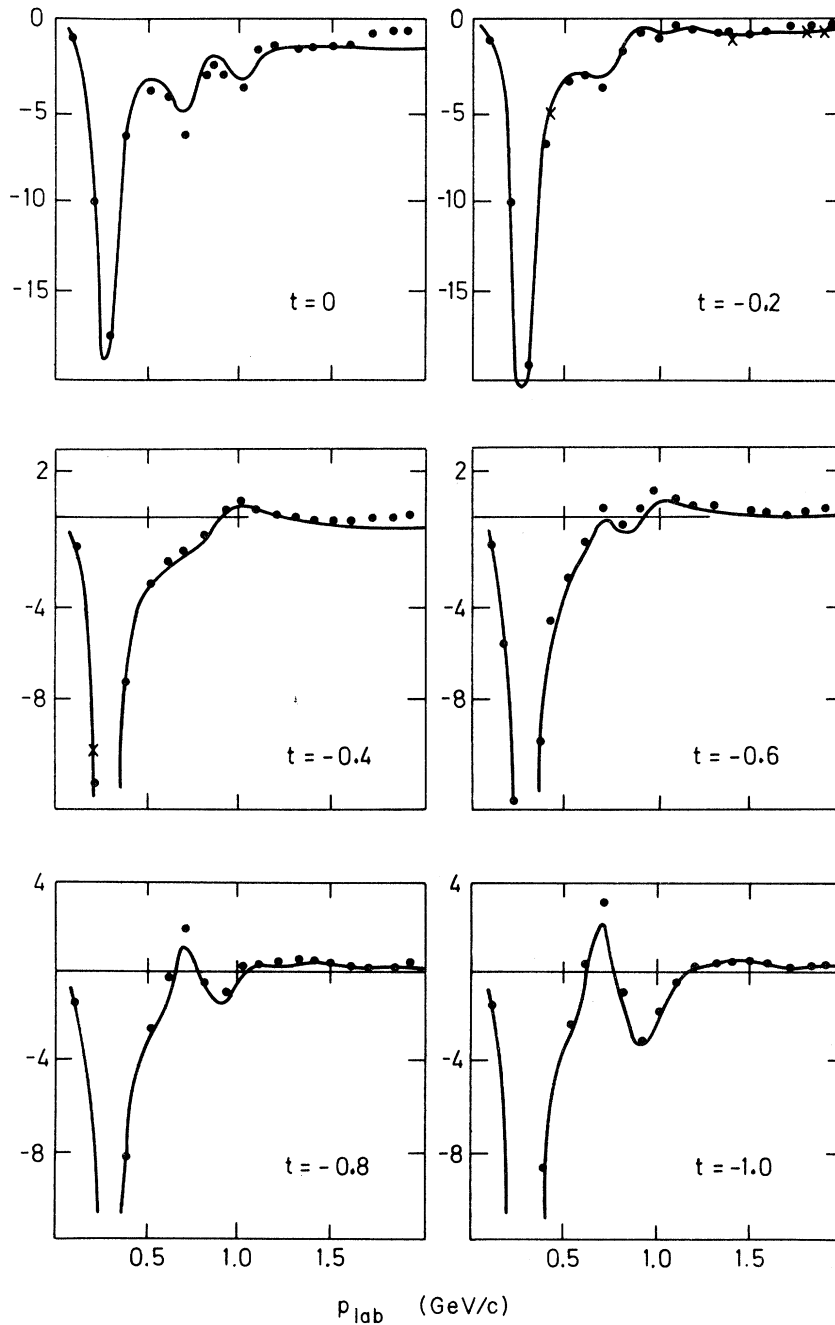


FIG. 7.  $\text{Im}B_{\text{CEX}}(\nu, t)$  in the notation of Fig. 4.

this is true even when we use Eq. (4.8) for the Pomeron.

### V. SUMMARY AND CONCLUSIONS

We have fitted pion-nucleon charge-exchange data below 2 GeV/c, using fixed- $t$  dispersion relations and the hypothesis of two-component duality. Good fits were obtained, and the resulting amplitudes are in agreement with recent  $\pi N$  phase-shift

analysis.<sup>19</sup> Predictions for the crossing-even amplitude  $B^+(\nu, t)$  obtained using the Barger-Phillips form for the Pomeron are also compatible with the phase-shift results, whereas those for  $A'^+(\nu, t)$  show significant discrepancies. However, these can be removed to a large extent by suitably modifying the Pomeron contribution at low energies.

These results show that fixed- $t$  dispersion relations together with the two-component duality

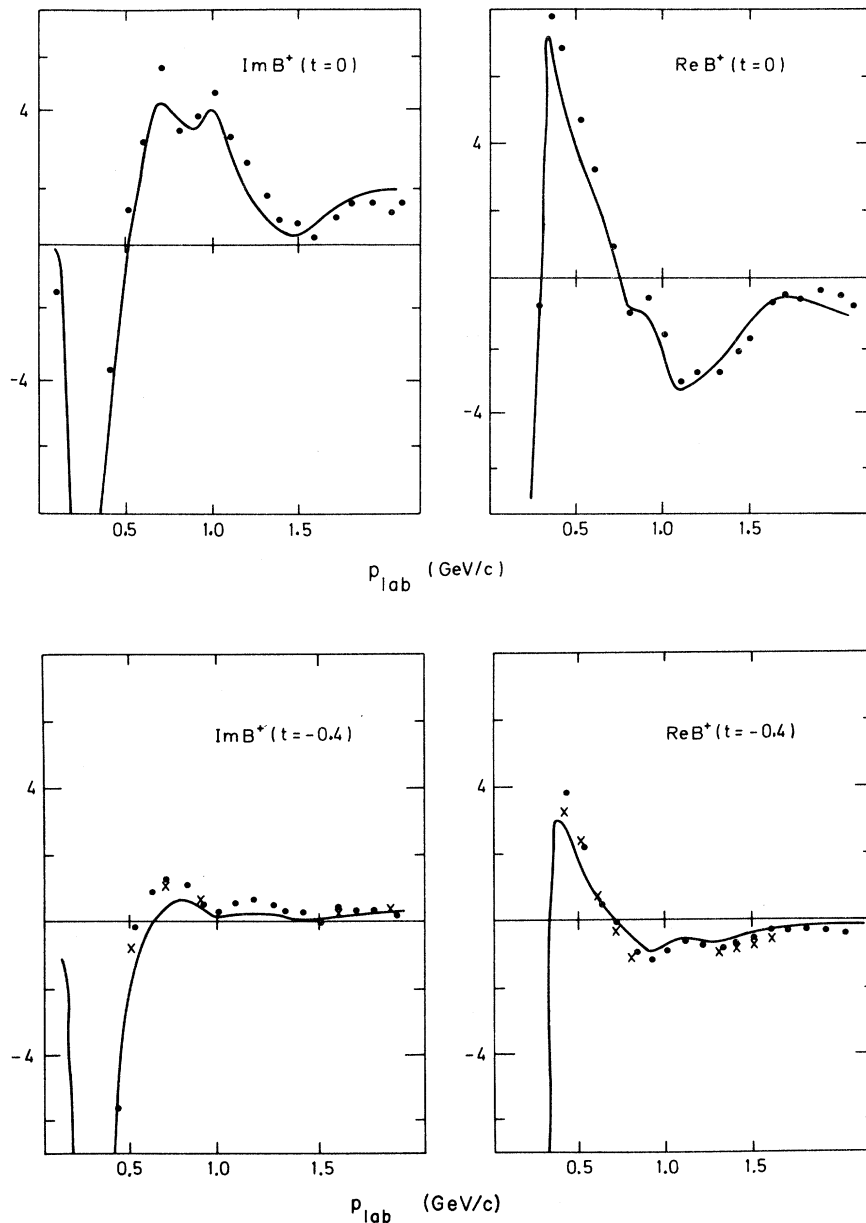


FIG. 8.  $B^+(\nu, t)$  for  $t=0$  and  $-0.4 \text{ GeV}^2$  in the notation of Fig. 4, obtained using the unmodified Barger-Phillips parametrization for the Pomeron.

hypothesis, provided an economical and theoretically satisfactory parametrization for analyzing data on two-body reactions. Work is in progress on analyzing data for  $\pi N \rightarrow K\Lambda$ .

We thank Dr. S. Almeded for assistance in interpreting the data compilation used in Ref. 19. We also thank the Rutherford High Energy Laboratory for providing computing facilities.

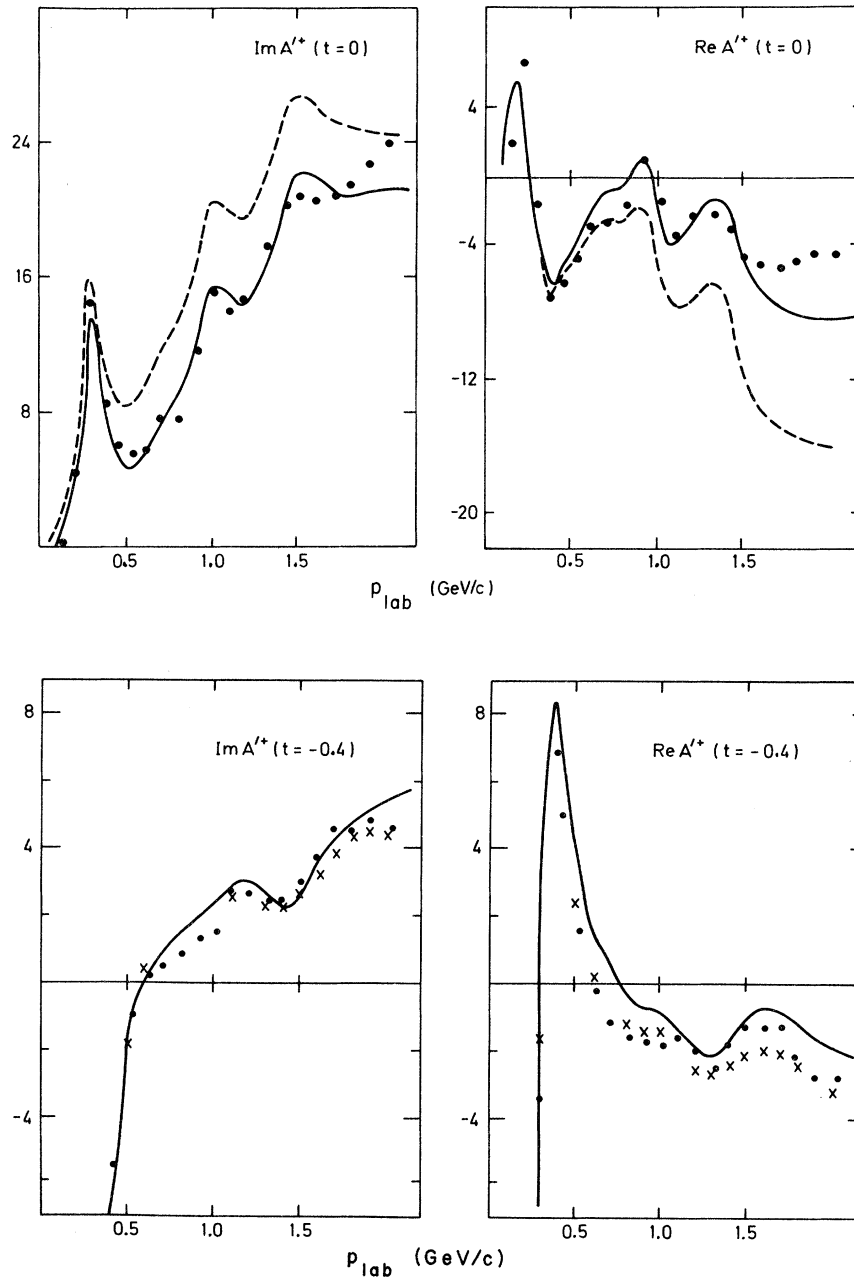


FIG. 9. (a) (upper diagrams).  $\text{Re}A^{*+}(\nu, t=0)$  and  $\text{Im}A^{*+}(\nu, t=0)$  obtained using the unmodified Barger-Phillips parametrization for the Pomeron (dashed curves), and using the modified form (solid curves). (b) (lower diagrams).  $\text{Re}A^{*+}(\nu, t=-0.4)$  and  $\text{Im}A^{*+}(\nu, t=-0.4)$  obtained using the unmodified Barger-Phillips parametrizations for the  $P$  and  $P'$ .

- <sup>1</sup>P. G. O. Freund, Phys. Rev. Lett. 20, 235 (1968); H. Harari, *ibid.* 20, 1395 (1968).
- <sup>2</sup>H. Harari and Y. Zarmi, Phys. Rev. 187, 2230 (1969).
- <sup>3</sup>M. Fukugita and T. Inami, Nucl. Phys. B44, 490 (1972).
- <sup>4</sup>R. C. Johnson, Phys. Rev. 183, 1406 (1969); D. R. Dance and G. Shaw, Phys. Lett. 28B, 182 (1968).
- <sup>5</sup>J. Hamilton and W. S. Woolcock, Rev. Mod. Phys. 35, 737 (1963).
- <sup>6</sup>B. R. Martin and G. D. Thompson, Nucl. Phys. B22, 285 (1970).
- <sup>7</sup>R. C. E. Devenish and D. H. Lyth, Phys. Rev. D 5, 47 (1972); Nucl. Phys. B43, 228 (1972).
- <sup>8</sup>G. I. Ghandour and R. G. Moorhouse, Phys. Rev. D 6, 856 (1972).
- <sup>9</sup>E. N. Argyres and A. P. Contogouris, Phys. Rev. D 6, 2018 (1972); M. F. Coirier *et al.*, Nucl. Phys. B44, 157 (1972).
- <sup>10</sup>I. Barbour, W. Malone, and R. G. Moorhouse, Phys. Rev. D 4, 1521 (1971); M. Hontebeyrie, J. Procureur, and Ph. Salin, Nucl. Phys. B55, 83 (1973).
- <sup>11</sup>E. Pietarinen, Nuovo Cimento 12A, 522 (1972).
- <sup>12</sup>R. G. Moorhouse and H. Oberlack, Phys. Lett. 43B, 44 (1973).
- <sup>13</sup>R. L. Walker, Phys. Rev. 182, 1729 (1969).
- <sup>14</sup>J. M. Blatt and V. F. Weisskopf, *Theoretical Nuclear Physics* (Wiley, New York, 1952).
- <sup>15</sup>A. A. Carter *et al.*, Nucl. Phys. B26, 445 (1971).
- <sup>16</sup>V. Barger and R. J. N. Phillips, Phys. Rev. 187, 2210 (1969).
- <sup>17</sup>F. Halzen and C. Michael, Phys. Lett. 36B, 367 (1971).
- <sup>18</sup>M. Hauser *et al.*, Phys. Lett. 35B, 252 (1971); P. Berardo *et al.*, Phys. Rev. D 6, 756 (1972); R. Hill *et al.*, *ibid.* 1, 729 (1970); R. Kurz, LBL Report No. UCRL 10564, 1962; D. Lind *et al.*, Phys. Rev. 138, B1509 (1965); W. S. Risk and E. Kleckner, Bull. Am. Phys. Soc. 11, 36 (1966); E. Hyman *et al.*, Phys. Rev. 165, 1437 (1968); A. Muller *et al.*, Phys. Lett. 10, 349 (1964), P. Borgeaud *et al.*, *ibid.* 10, 134 (1964); A. Bigi *et al.*, Nuovo Cimento 34, 878 (1964); A. Weinberg *et al.*, Phys. Rev. Lett. 8, 70 (1962); V. V. Barmin *et al.*, Zh. Eksp. Teor. Fiz. 46, 142 (1964) [Sov. Phys.—JETP 19, 102 (1964)]; D. D. Drobnis *et al.*, Phys. Rev. Lett. 20, 274 (1968); C. Chiu *et al.*, Phys. Rev. 187, 1827 (1969); A. Carroll *et al.*, *ibid.* 177, 2047 (1969).
- <sup>19</sup>S. Almeded and C. Lovelace, Nucl. Phys. B40, 157 (1972).
- <sup>20</sup>E. Bracci *et al.*, CERN Report No. CERN/HERA 72-1 (unpublished).
- <sup>21</sup>Particle Data Group, Phys. Lett. 39B, 1 (1972).
- <sup>22</sup>A. T. Davies, Nucl. Phys. B21, 359 (1970).
- <sup>23</sup>G. Ebel *et al.*, Nucl. Phys. B33, 317 (1971).
- <sup>24</sup>K. Igi, Phys. Rev. Lett. 9, 76 (1962).

## Multiplicity, Gas Analog, Phase Transition, and the Dual Resonance Model\*

Richard C. Arnold, Stanley Fenster, and Gerald H. Thomas

High Energy Physics Division, Argonne National Laboratory, Argonne, Illinois 60439

(Received 31 May 1973)

The multiplicity distribution  $\sigma_N(s)$  for the Koba-Nielsen form of the dual-resonance model is computed in the limit of large  $N$  and  $s$ . It is noticed after simplifying approximations that  $\sigma_N(s)$  has the form of the absolute square  $|\Phi_N|^2$  of the statistical-mechanics partition function of  $N$  unit charges free to move on an infinitely thin circular wire. This partition function of a Coulomb gas has been evaluated by Dyson, and gives a closed-form estimate of  $\sigma_N(s)$ . Using this estimate, the properties of the multiplicity distribution are obtained. In the language of statistical mechanics, a first-order phase transition is found in the limit of infinitely narrow resonance widths. If the resonances are given finite widths, a second-order phase transition or critical point can occur. In the language of high-energy physics, these possibilities correspond to the second moment  $f_2 = \langle N(N-1) \rangle - \langle N \rangle^2$  increasing like  $(\ln s)^2$  or like  $(\ln s)^{1+\nu}$ ,  $0 < \nu < 1$ , respectively; the multiperipheral model predicts  $f_2 \sim \ln s$ , while two-component models predict  $f_2 \sim (\ln s)^2$ .

### I. INTRODUCTION

One of the distributions most easily obtained in high-energy hadron collisions above 100 GeV/c is the multiplicity of charged secondary particles.<sup>1</sup> If  $n$  is the number of charged prongs, and  $\sigma_n$  the cross section associated with that multiplicity, the multiplicity distribution is given by  $(\sigma_n/\sigma_{\text{tot}})$ . If particles were produced in a statistically independent fashion this distribution would be Poisson in

$n$ . Such a distribution is not far from what is experimentally observed in collisions at 50 and 70 GeV/c (see Ref. 2) but at higher energies the distribution is observed to be broader; large deviations are seen that indicate strong (positive) correlations.

The description of multiplicity distributions, and their comparison with theoretical models, is greatly facilitated by the employment of the language (but not necessarily the physics) of statisti-